Supporting Information for

A Lumped Pathway Metabolic Model of Organic Carbon Accumulation and Mobilization by the Alga *Chlamydomonas reinhardtii*

J.S. Guest, M.C.M. van Loosdrecht, S.J. Skerlos, N.G. Love*

List of Tables (Pages S2-S6)

List of Figures (Pages S7-S10)

Table S1. Summary of reactions included in the metabolic model, normalized to a C-mole basis.

Rate	Reaction	Stoichiometry	Citations
$\mathbf{R_1}$	Synthesis of G3P from CO_2	$\alpha_p\ h\nu + CO_2 \rightarrow {}^1/_3\ G3P + O_2$	[1, 2]
$\mathbf{R_2}$	Synthesis of acetyl-CoA from G3P	${}^1/_3\ G3P \rightarrow {}^1/_3$ acetyl-CoA + ${}^2/_3\ NADH_2 + {}^2/_3\ ATP + {}^1/_3\ CO_2$	[3, 4]
$\mathbf{R_3}$	Synthesis of biomass precursors from acetyl-CoA	$\frac{1}{2}(1 + \delta_x + \delta_N)$ acetyl-S-CoA + $0.2\ NO_3^-$ + $(\alpha_m - \frac{1}{2}\delta_N)$ ATP $\rightarrow CH_{1.8}O_{0.5}N_{0.2} + (\delta_x + \delta_N)\ CO_2 + (2\ \delta_x - 0.1)\ NADH_2$	[5, 6]
$\mathbf{R_4}$	Polymerization of biomass precursors & maintenance	$CH_{1.8}O_{0.5}N_{0.2} + \left(\alpha_X + \frac{m_{ATP}}{\mu}\right)$ ATP $\rightarrow \frac{1}{n}(CH_{1.8}O_{0.5}N_{0.2})_n$	[6, 7]
$\mathbf{R_5}$	Carbon source catabolism	${}^1/_2$ acetyl-CoA $\rightarrow 1\ CO_2 + {}^3/_2\ NADH_2 + {}^1/_2\ FADH_2 + {}^1/_2\ ATP$	[4]
$\mathbf{R_6}$	Oxidative phosphorylation	$1\ NADH_2 + {}^1/_2\ O_2 \rightarrow \delta_{PO}\ ATP$	[8, 9]
$\mathbf{R_7}$	Synthesis of PG from G3P	${}^1/_3\ G3P + {}^1/_6\ (glucose)_n + {}^1/_6\ ATP \rightarrow {}^1/_6\ (glucose)_{n+1}$	[3, 4]
$\mathbf{R_8}$	Synthesis of G3P from PG	${}^1/_6\ (glucose)_{n+1} + {}^1/_6\ ATP \rightarrow {}^1/_6\ (glucose)_n + {}^1/_3\ G3P$	[10]
$\mathbf{R_9}$	Synthesis of TAG from acetyl-CoA	${}^{25}/_{51}$ acetyl-CoA + ${}^{23}/_{51}\ ATP + {}^{42}/_{51}\ NADPH_2 + {}^3/_{51}\ NADH_2 + {}^1/_{51}\ CO_2 \rightarrow {}^1/_{51}\ TAG$	[3, 11]
$\mathbf{R_{10}}$	Synthesis of acetyl-CoA from TAG	${}^1/_{51}\ TAG + {}^2/_{51}\ ATP \rightarrow {}^{24}/_{51}\ NADH_2 + {}^{21}/_{51}\ FADH_2 + {}^1/_{51}\ CO_2 + {}^{25}/_{51}$ acetyl-CoA	[4, 10]

Note: α_p in R_1 is a light energy efficiency factor [unitless].

Table S2. Linear equations for nutrient-available metabolism of X_{CPO}.

#	Equation	Units
1[a]	$r_{NADH2} = 0 = {}^{2}/_{3}\, r_2 + (2\delta_X - 0.1)\, r_3 + {}^{11}/_{6}\, r_5 - r_6 + {}^{38}/_{51}\, r_{10}$	moles-($NADH_2$)·hour^{-1}
2	$r_{ATP} = 0 = {}^{2}/_{3}\, r_2 - (\alpha_m - \tfrac{1}{2}\,\delta_N)\, r_3 - \left(\alpha_X + \frac{m_{ATP}}{\mu}\right) r_4 + {}^{1}/_{2}\, r_5 + \delta_{PO}\, r_6 - {}^{1}/_{6}\, r_8 - {}^{2}/_{51}\, r_{10}$	moles-(ATP)·hour^{-1}
3	$r_{precursors} = 0 = r_3 - r_4$	moles-(precursors as C)·hour^{-1}
4	$r_{acetyl\text{-}CoA} = 0 = {}^{2}/_{3}\, r_2 - (1 + \delta_x + \delta_N)\, r_3 - r_5 + {}^{50}/_{51}\, r_{10}$	moles-(acetyl-CoA as C)·hour^{-1}
5	$r_{G3P} = 0 = r_1 - r_2 + r_8$	moles-(G3P as C)·hour^{-1}
6	$r_{XCPO} = r_4$	moles-(X_{CPO} as C) ·hour^{-1}
7	$r_{PG} = - r_8$	moles-(PG as C)·hour^{-1}
8	$r_{TAG} = - r_{10}$	moles-(TAG as C)·hour^{-1}
9	$r_{O2} = r_1 - {}^{1}/_{2}\, r_6$	moles-(O_2)·hour^{-1}
10	$r_{CO2} = - r_1 + {}^{1}/_{3}\, r_2 + (\delta_x + \delta_N)\, r_3 + r_5 + {}^{1}/_{51}\, r_{10}$	moles-(CO_2)·hour^{-1}
11[b]	$4\, r_1 + 4\,(-{}^{1}/_{2}\, r_6) = {}^{290}/_{51}\, r_{TAG} + 4\, r_{PG} + 5.8\, r_{XCPO}$	-

[a] Assumes $FADH_2 = {}^{2}/_{3}\, NADH_2$.
[b] Degree of reduction balance based on Roels[5] assuming a TAG elemental composition of $C_{51}H_{98}O_6$. Carbon in functional biomass (X_{CPO}) is reduced 21/5 and nitrogen 8/5 (total of 29/5).

Table S3. Linear equations for nutrient-deplete metabolism of X_{CPO}.

#	Equation	Units
1[a]	$r_{NADH2} = 0 = {}^{2}/_{3}\, r_2 + (2\delta_X - 0.1)\, r_3 + {}^{11}/_{6}\, r_5 - r_6 - {}^{45}/_{51}\, r_9$	moles-($NADH_2$)·hour^{-1}
2	$r_{ATP} = 0 = {}^{2}/_{3}\, r_2 - (\alpha_m - \tfrac{1}{2}\,\delta_N)\, r_3 - \left(\alpha_X + \frac{m_{ATP}}{\mu}\right) r_4 + {}^{1}/_{2}\, r_5 + \delta_{PO}\, r_6 - {}^{1}/_{6}\, r_7 - {}^{23}/_{51}\, r_9$	moles-(ATP)·hour^{-1}
3	$r_{precursors} = 0 = r_3 - r_4$	moles-(precursors as C)·hour^{-1}
4	$r_{acetyl\text{-}CoA} = 0 = {}^{2}/_{3}\, r_2 - (1 + \delta_x + \delta_N)\, r_3 - r_5 - {}^{50}/_{51}\, r_9$	moles-(acetyl-CoA as C)·hour^{-1}
5	$r_{G3P} = 0 = r_1 - r_2 - r_7$	moles-(G3P as C)·hour^{-1}
6	$r_{XCPO} = r_4$	moles-(X_{CPO} as C) ·hour^{-1}
7	$r_{PG} = r_7$	moles-(PG as C)·hour^{-1}
8	$r_{TAG} = r_9$	moles-(TAG as C)·hour^{-1}
9	$r_{O2} = r_1 - {}^{1}/_{2}\, r_6$	moles-(O_2)·hour^{-1}
10	$r_{CO2} = - r_1 + {}^{1}/_{3}\, r_2 + (\delta_x + \delta_N)\, r_3 + r_5 - {}^{1}/_{51}\, r_9$	moles-(CO_2)·hour^{-1}
11[b]	$4\, r_1 + 4\,(-{}^{1}/_{2}\, r_6) = {}^{290}/_{51}\, r_{TAG} + 4\, r_{PG} + 5.8\, r_{XCPO}$	-

[a] Assumes $FADH_2 = {}^{2}/_{3}\, NADH_2$.
[b] Degree of reduction balance based on Roels[5], assuming a TAG elemental composition of $C_{51}H_{98}O_6$.

Table S4. Linear equation solutions for nutrient-available and nutrient-deplete metabolisms.

Description [Units]	Nutrient-Available Metabolism	Nutrient-Deplete Metabolism
Specific Rate of Photosynthesis [moles-(CO_2 fixed to G3P)·mole-(X_{CPO} as C)$^{-1}$·hour^{-1}]	$q_{PHOT}^{NR} = \frac{\mu^{NR}}{Y_{XCPO}^{NR}} + \frac{q_{CH}^{NR}}{Y_{CH}^{NR}} + \frac{q_{LI}^{NR}}{Y_{LI}^{NR}} + \frac{m_{ATP}^{NR}}{Y_{ATP}^{NR}}$	$q_{PHOT}^{ND} = \frac{\mu^{ND}}{Y_{XCPO}^{ND}} + \frac{q_{CH}^{ND}}{Y_{CH}^{ND}} + \frac{q_{LI}^{ND}}{Y_{LI}^{ND}} + \frac{m_{ATP}^{ND}}{Y_{ATP}^{ND}}$
Specific Rate of CO_2 Production [moles-(CO_2)·mole-(X_{CPO} as C)$^{-1}$·hour^{-1}]	$q_{CO2}^{NR} = -\mu^{NR} - q_{CH}^{NR} - q_{LI}^{NR}$	$q_{CO2}^{ND} = -\mu^{ND} - q_{CH}^{ND} - q_{LI}^{ND}$
Specific Rate of O_2 Production [moles-(O_2)·mole-(X_{CPO} as C)$^{-1}$·hour^{-1}]	$q_{O2}^{NR} = \frac{1479}{1020}\,\mu^{NR} + q_{CH}^{NR} + \frac{145}{102} q_{LI}^{NR}$	$q_{O2}^{ND} = \frac{1479}{1020}\,\mu^{ND} + q_{CH}^{ND} + \frac{145}{102} q_{LI}^{ND}$

Note: The coefficient in front of the μ in the O_2 production calculations would be 1071/1020 rather than 1479/1020 if ammonia were the nitrogen source.

q_{CO2}; specific rate of net CO_2 production, moles-(CO_2 as C)·mole-(X_{CPO} as C)$^{-1}$·hr^{-1}

q_{O2}; specific rate of net O_2 production, moles-(O_2)·mole-(X_{CPO} as C)$^{-1}$·hr^{-1}

q_{phot}; specific rate of CO_2 fixation to G3P, moles-(G3P as C)·mole-(X_{CPO} as C)$^{-1}$·hr^{-1}

Table S5. Stoichiometric yields derived from linear equation solutions.

Description [Units]	Nutrient-Available Metabolism	Nutrient-Deplete Metabolism
yield of PG on CO_2 fixed to G3P [(C-moles PG)·(C-mole CO_2 fixed to G3P)$^{-1}$]	$Y_{CH}^{NR} = \frac{18 + 34\,\delta_{PO}}{15 + 34\,\delta_{PO}}$	$Y_{CH}^{ND} = \frac{18 + 34\,\delta_{PO}}{21 + 34\,\delta_{PO}}$
yield of TAG on CO_2 fixed to G3P [(C-moles TAG)·(C-mole CO_2 fixed to G3P)$^{-1}$]	$Y_{LI}^{NR} = \frac{153 + 289\,\delta_{PO}}{69 + 389\,\delta_{PO}}$	$Y_{LI}^{ND} = \frac{153 + 289\,\delta_{PO}}{144 + 410\,\delta_{PO}}$
yield of biomass on CO_2 fixed to G3P [(C-moles biomass)·(C-mole CO_2 fixed to G3P)$^{-1}$]	$Y_{XCPO}^{NR} = Y_{XCPO}^{ND} = \frac{90 + 170\delta_{PO}}{45 + 90\,\alpha_m + 90\,\alpha_X + 174\,\delta_{PO} + 165\,\delta_{PO}\delta_N + 45\,\delta_X - 15\,\delta_{PO}\delta_X}$	
yield of ATP on CO_2 fixed to G3P [(moles of ATP)·(C-mole CO_2 fixed to G3P)$^{-1}$]	$Y_{ATP}^{NR} = Y_{ATP}^{ND} = \frac{9 + 17\,\delta_{PO}}{9}$	

Note: The coefficient in front of the μ in the O_2 production calculations would be 1071/1020 rather than 1479/1020 if ammonia were the nitrogen source.

Table S6. Stoichiometric matrix linking transformation processes (rows) to state variables (columns).

	State Variable									
	R	**X_{CPO}**	**X_{CH}**	**X_{LI}**	**S_{CO2}**	**S_{O2}**	**S_{NO}***	**S_P***	**X_N**	**X_P**
Process	g-(Chl)·g-(C)$^{-1}$	moles-(C)·L^{-1}	moles-(C)·L^{-1}	moles-(C)·L^{-1}	moles-(C)·L^{-1}	moles-(O_2)·L^{-1}	moles-(N)·L^{-1}	moles-(P)·L^{-1}	moles-(N)·L^{-1}	moles-(P)·L^{-1}
Photoadaptation (P_1)	1									
Nitrate Uptake (P_2)							-1		1	
Phosphorus Uptake (P_3)								-1		1
Photoautotrophic Growth (P_4)		1			-1	$\frac{1479}{1020}$			$-Q_{N,min}$	$-Q_{P,min}$
Growth on Stored Carbohydrates (P_5)		1	$-\frac{Y_{CH}^{NR}}{Y_{XCPO}}$		$\frac{Y_{CH}^{NR}}{Y_{XCPO}}-1$	$-\frac{Y_{CH}^{NR}}{Y_{XCPO}}+\frac{1479}{1020}$			$-Q_{N,min}$	$-Q_{P,min}$
Growth on Stored Lipids (P_6)		1		$-\frac{Y_{LI}^{NR}}{Y_{XCPO}}$	$\frac{Y_{LI}^{NR}}{Y_{XCPO}}-1$	$-\frac{Y_{LI}^{NR}}{Y_{XCPO}}\frac{145}{102}+\frac{1479}{1020}$			$-Q_{N,min}$	$-Q_{P,min}$
Stored Carbohydrate Degradation for Maintenance (P_7)			-1		1	-1				
Stored Lipid Degradation for Maintenance (P_8)				-1	1	$-\frac{145}{102}$				
Endogenous Respiration (P_9)		-1			1	$-\frac{1479}{1020}$			**	**
Carbohydrate Storage (P_{10})			1		-1	1				
Lipid Storage (P_{11})				1	-1	$\frac{145}{102}$				

* S_{NO} and S_P are presented in this table on a molar basis for clarity. The model is executed using molar values, but parameters are converted to mass units in the text to be consistent with medium preparation procedures and other published models.

** It was assumed X_{CPO}-associated nitrogen and phosphorus were bioavailable after endogenous respiration. Inert material (including inert N and P) was not included in this model formulation.

Table S7. Fixed stoichiometric and kinetic parameters used in PPM calibration.

Parameter	Description	Value	Units
Stoichiometric Parameters			
δ_x	CO_2 production from the synthesis of 1 C-mole of biomass precursors from acetyl-CoA	0.266[a]	C-moles of CO_2 produced per C-mole of X_{CPO}
δ_N	CO_2 production from the catabolism of acetyl-CoA to generate reducing power for NO_3^- reduction for assimilation	0.436[b]	C-moles of CO_2 produced per C-mole of X_{CPO}
α_M	ATP requirement for synthesis of biomass precursors from acetyl-CoA	0.66[c]	moles ATP per C-mole of X_{CPO}
α_X	ATP required for polymerization of biomass precursors (monomers) to functional biomass	1.5[d]	moles of ATP per C-mole of X_{CPO}
δ_{PO}	efficiency of oxidative phosphorylation (P/O ratio) in mitochondria	2.0[e]	moles of ATP produced per mole of $NADH_2$ oxidized
Kinetic Parameters			
I_{OPT}	optimal irradiance	300	$\mu E \cdot m^{-2} \cdot s^{-1}$
K_γ	photoadaptation coefficient	10^{-5}	(unitless)
K_{NO}	half-saturation coefficient for nitrogen	0.1	$mg\text{-}(N) \cdot L^{-1}$
K_P	half-saturation coefficient for phosphorus	1	$mg\text{-}(P) \cdot L^{-1}$
K_{STO}	half-saturation coefficient for stored organic carbon	1.6	$moles\text{-}(X_{CH}$ as C$) \cdot mole\text{-}(X_{CPO}$ as C$)^{-1}$

[a] Acetate via the glyoxylate cycle and isocitrate-lyase.[12]

[b] Calculated based on the molar ratio of 0.2 moles of N required per C-mole of biomass formed and the requirement of 8 electrons per mole of N reduced from NO_3^- to NH_3. Reducing power was assumed to be generated via acetyl-CoA catabolism (R_5). The value for δ_N assumes the reducing power was generated via catabolism, R_5, and ATP generated during catabolism offsets ATP needs during polymerization of functional biomass, R_3.

[c] [9], consistent with assumption by [6].

[d] [7], consistent with assumption by [6].

[e] [13].

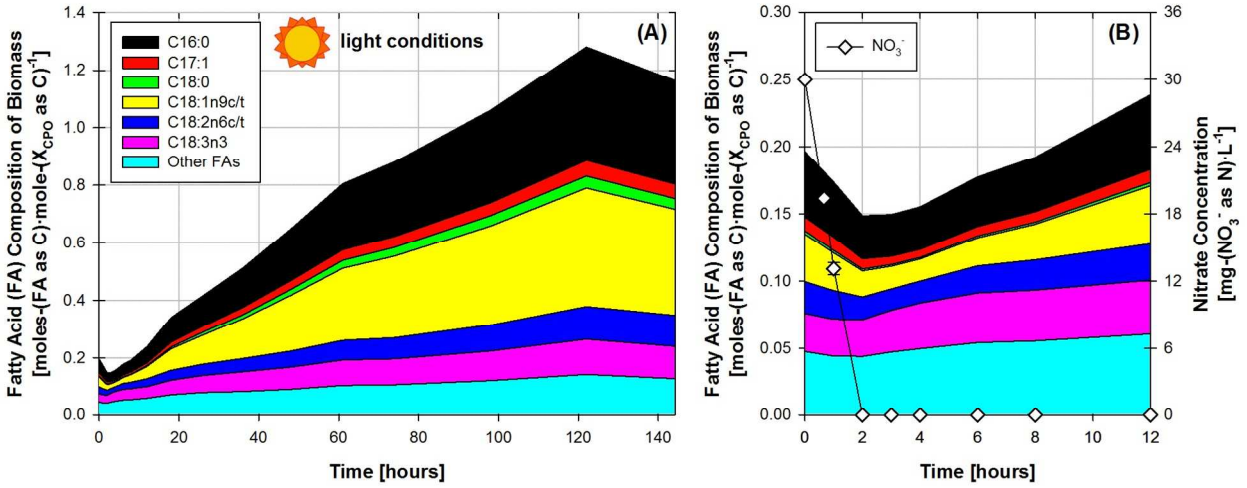

Figure S1. Fatty acid (FA) content of biomass (where "biomass" includes $X_{CPO} + X_{LI} + X_{CH}$) over time. Data shown is for PBR 3 in batch operation under light conditions, with an initial spike of 30 mg-(N)·L^{-1}. Two timescales are shown: (A) the full duration of the 144 hour study and (B) a closer view of the first 12 hours with nitrate data overlayed. Note that these values include FAs associated with X_{CPO} as well as the FAs associated with X_{LI}.

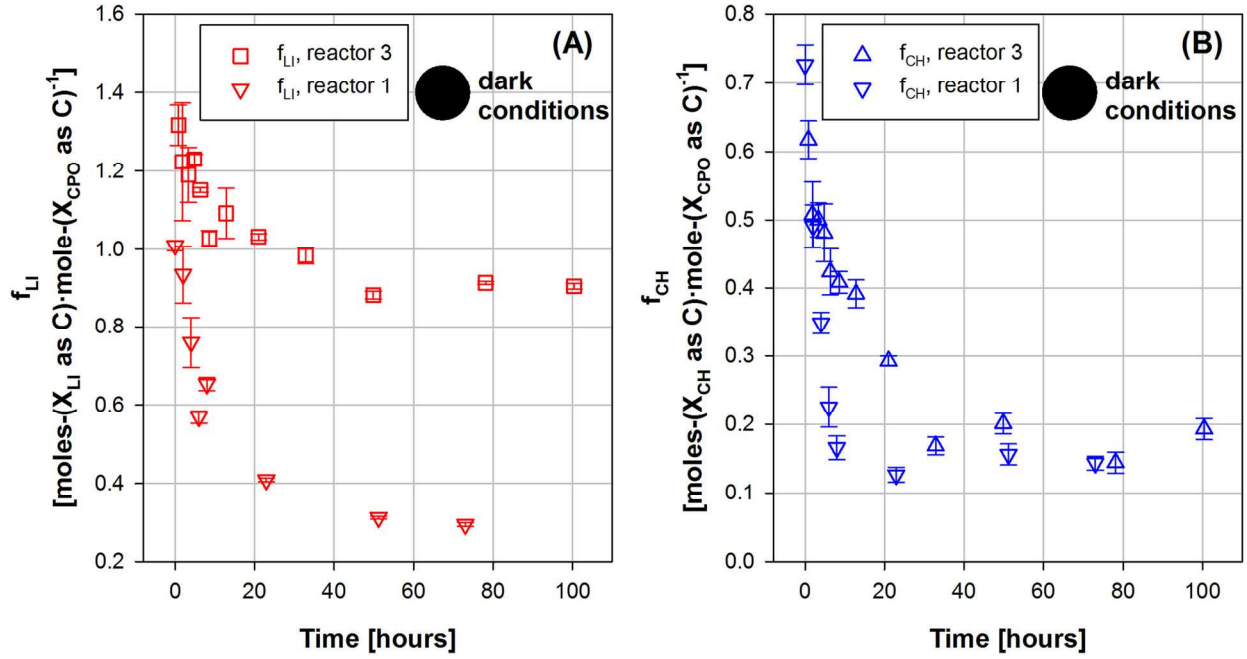

Figure S2. Experimental data demonstrating (A) f_{LI} and (B) f_{CH} reduction under dark, nutrient-available conditions for PBRs 1 and 3. Although the extent of X_{CH} mobilization (i.e., the final f_{CH} value) was consistent across reactors, the extent of X_{LI} mobilization varied.

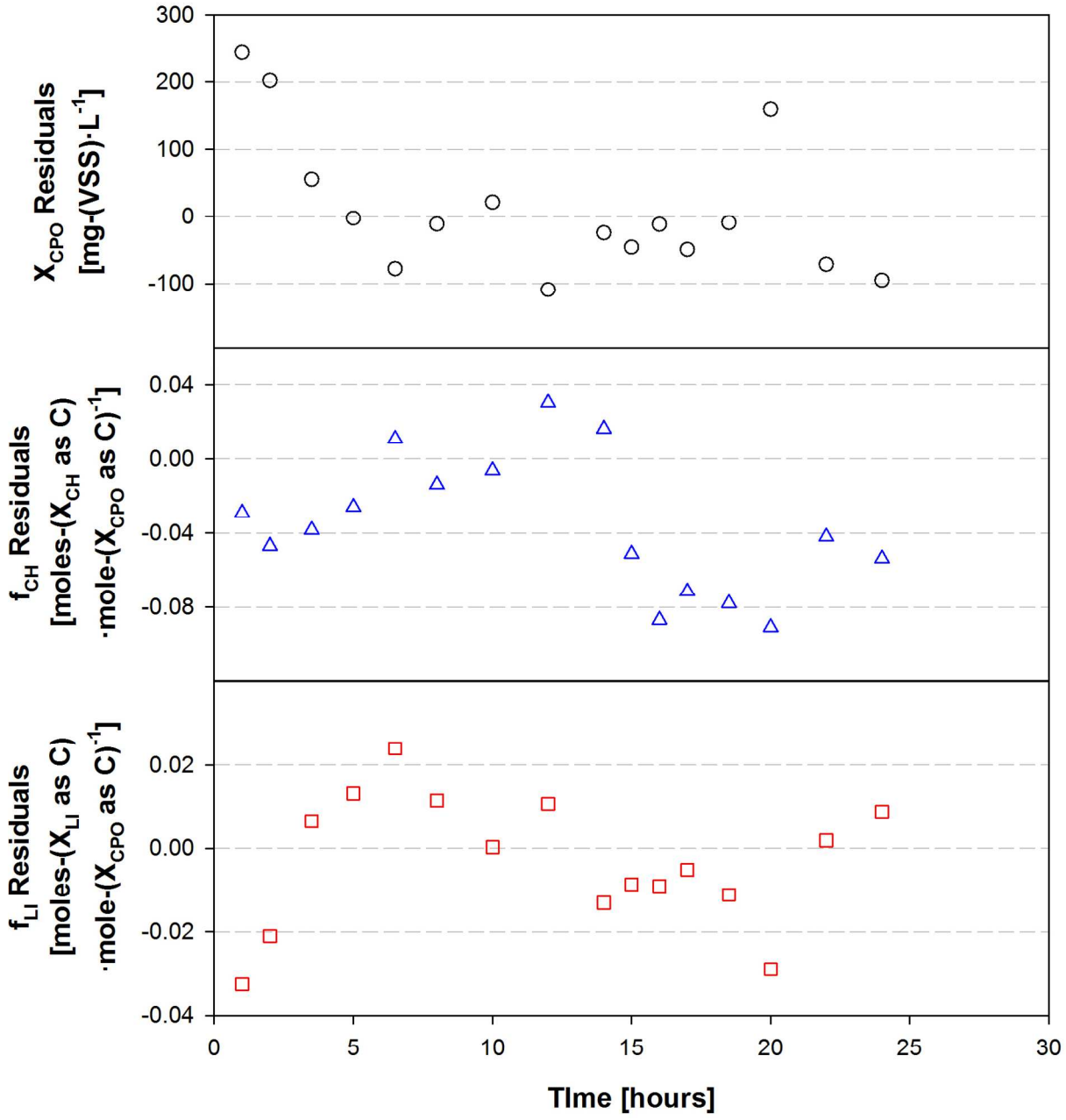

Figure S3. Plots of X_{CPO} (top), f_{CH} (middle) and f_{LI} (bottom) residuals (y-axes) versus time (x-axis) for validation study (Residual = Experimental Value – Model Predicted Value).

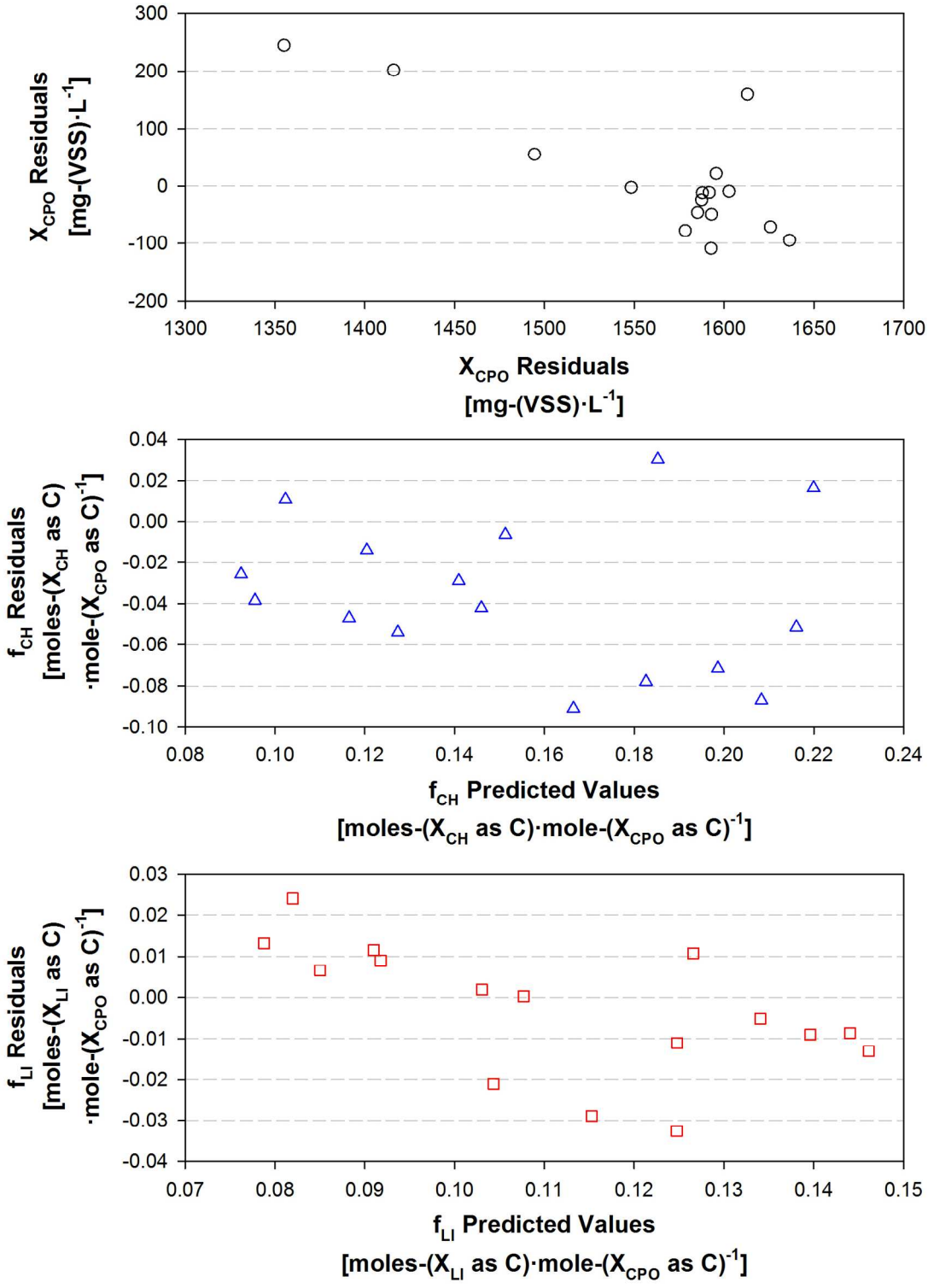

Figure S4. Plots of X_{CPO} (top), f_{CH} (middle) and f_{LI} (bottom) residuals (y-axes) versus model predicted values (x-axes) from validation experiment (Residual = Experimental Value – Model Predicted Value).

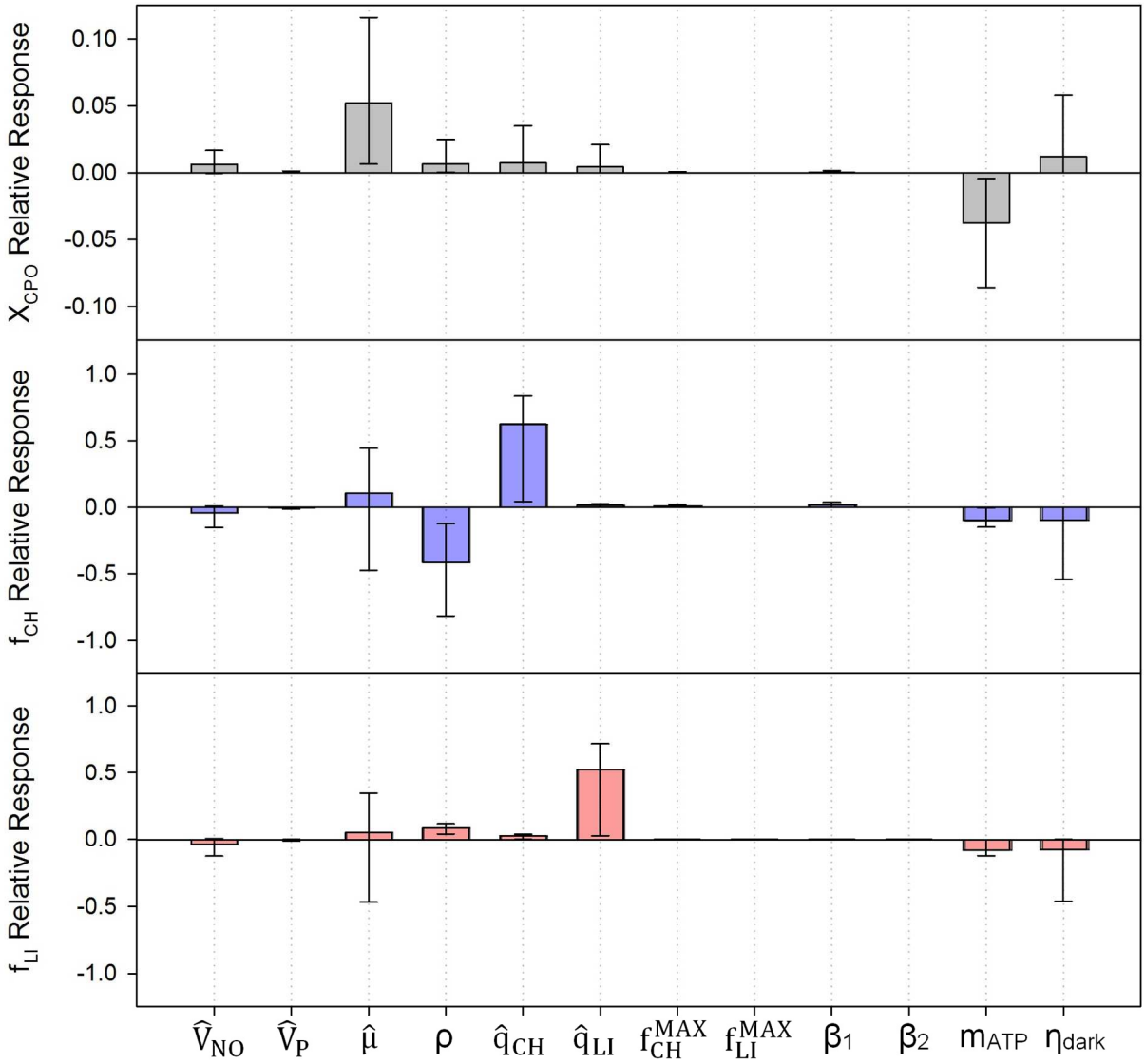

Figure S5. Sensitivity analysis results for X_{CPO} (top), f_{CH} (middle) and f_{LI} (bottom). Each parameter was changed by +/- 10% and model outputs (X_{CPO}, f_{CH}, f_{LI}) from validation study were analyzed. Relative responses of model outputs were calculated as % change in output value divided by % change in input parameter (a relative response of 1 would represent a 10% change in model outputs in response to a 10% change in the value of an input parameter). Bars represent average relative response across the full validation study. Error bars extend to maximum and minimum change for any given timepoint. Note that the scale for the top figure (X_{CPO}) is 1/10 that of the other two figures.

References

1. Alric, J., Cyclic electron flow around photosystem I in unicellular green algae. *Photosynth. Res.* **2010,** *106*, (1-2), 47-56.
2. Peltier, G.; Tolleter, D.; Billon, E.; Cournac, L., Auxiliary electron transport pathways in chloroplasts of microalgae. *Photosynth. Res.* **2010,** *106*, (1-2), 19-31.
3. Boyle, N. R.; Morgan, J. A., Flux balance analysis of primary metabolism in *Chlamydomonas reinhardtii*. *BMC Syst. Biol.* **2009,** *3*.
4. Manichaikul, A.; Ghamsari, L.; Hom, E. F. Y.; Lin, C. W.; Murray, R. R.; Chang, R. L.; Balaji, S.; Hao, T.; Shen, Y.; Chavali, A. K.; Thiele, I.; Yang, X. P.; Fan, C. Y.; Mello, E.; Hill, D. E.; Vidal, M.; Salehi-Ashtiani, K.; Papin, J. A., Metabolic network analysis integrated with transcript verification for sequenced genomes. *Nat. Methods* **2009,** *6*, (8), 589-592.
5. Roels, J. A., Application of macroscopic principles to microbial metabolism. *Biotechnol. Bioeng.* **1980,** *22*, (12), 2457-2514.
6. van Aalst-van Leeuwen, M. A.; Pot, M. A.; van Loosdrecht, M. C. M.; Heijnen, J. J., Kinetic modeling of poly(beta-hydroxybutyrate) production and consumption by *Paracoccus pantotrophus* under dynamic substrate supply. *Biotechnol. Bioeng.* **1997,** *55*, (5), 773-782.
7. Verduyn, C.; Stouthamer, A. H.; Scheffers, W. A.; Vandijken, J. P., A theoretical evaluation of growth yields of yeasts. *Antonie Van Leeuwenhoek Int. J. Gen. Mol. Microbiol.* **1991,** *59*, (1), 49-63.
8. Roels, J. A., *Energetics and Kinetics in Biotechnology*. Elsevier Biomedical Press BV: Amsterdam, The Netherlands, 1983; p 330.
9. Stouthamer, A. H., A theoretical study on the amount of ATP required for synthesis of microbial cell material. *Antonie Van Leeuwenhoek* **1973,** *39*, (3), 545-565.
10. Nelson, D. L.; Cox, M. M., *Lehninger Principles of Biochemistry, Fourth Edition*. W.H. Freeman: 2004; p 1,100.
11. Hu, Q.; Sommerfeld, M.; Jarvis, E.; Ghirardi, M.; Posewitz, M.; Seibert, M.; Darzins, A., Microalgal triacylglycerols as feedstocks for biofuel production: Perspectives and advances. *Plant J.* **2008,** *54*, 621-639.
12. Gommers, P. J. F.; Vanschie, B. J.; Vandijken, J. P.; Kuenen, J. G., Biochemical limits to microbial growth yields: an analysis of mixed substrate utilization. *Biotechnol. Bioeng.* **1988,** *32*, (1), 86-94.
13. Noctor, G.; Foyer, C. H., Homeostasis of adenylate status during photosynthesis in a fluctuating environment. *J. Exp. Bot.* **2000,** *51*, 347-356.